Contrib Mineral Petrol (2013) 165:477–493
DOI 10.1007/s00410-012-0818-5

ORIGINAL PAPER

Mineralogical and geochemical investigation of layered chromitites from the Bracco–Gabbro complex, Ligurian ophiolite, Italy

R. J. Baumgartner · F. Zaccarini · G. Garuti · O. A. R. Thalhammer

Received: 29 April 2012 / Accepted: 21 September 2012 / Published online: 10 October 2012

Abstract The Bracco–Gabbro Complex (Internal Liguride ophiolite), that intruded subcontinental mantle peridotite, contains layers of chromitite that are associated with ultramafic differentiates. The chromitites and disseminated chromites in the ultramafics have Al contents similar to the Al-rich podiform chromitites [$0.40 < Cr\# = Cr/(Cr + Al) < 0.55$]. TiO_2 contents of the chromitites are unusually high and range up to 0.82 wt%. The calculated Al_2O_3 and TiO_2 content of the parental melt suggest that the melt was a MORB type. Geothermobarometrical calculations on few preserved silicate inclusions revealed formation temperatures between 970 and 820 °C under a relatively high oxygen fugacity ($\Delta \log fO_2$ at +2.0–2.4). Chromitites were altered during the post-magmatic tectono-metamorphic uplift and the final exposure at the seafloor, as evidenced by the formation of ferrian chromite. The PGE contents of the chromitites and associated ultramafics are unusually low (PGEmax 83 ppb). The chondrite-normalized PGE spidergrams show positive PGE patterns and to some extent similarities with the typical trend of stratiform chromitites. No specific PGM have been found but low concentrations of PPGE (Rh, Pt, and Pd) have been detected in the sulphides that occur interstitially to or enclosed in chromite. Recently, it has been shown that the Internal Liguride gabbroic intrusions have formed by relatively low degrees of partial melting of the asthenospheric mantle. We conclude that the low degree of partial melting might be the main factor to control the unusual low PGE contents and the rather unique PGE distribution in the Bracco chromitites.

Keywords Ligurian ophiolite · Bracco–Gabbro complex · Layered chromitites · Platinum-group elements · Silicate inclusions · Geothermobarometry

Introduction

Refractory chromite is one of the early stable phases to crystallize from mafic to ultramafic melts and is therefore a common accessory mineral in mafic to ultramafic magmatic rocks. Rocks containing more than 45 % modal chromite are classified as chromitites. Chromitites are associated with layered igneous intrusions in tectonically stable continental crust as well as with ultramafic to mafic complexes in orogenic belts, for example ophiolites, orogenic lherzolites and concentrically zoned complexes of the Ural–Alaskan type (Thayer 1970; Stowe 1994; Garuti et al. 2012). According to the morphology of the ore body, chromitites are classified into two descriptive types: (i) the stratiform chromitites consist of extended layers of massive chromite associated with ultramafic cumulates in the lower part of continental layered intrusions and supra-Moho cumulate sequences of ophiolites, (ii) the podiform chromitites consist of lenticular and irregular ore bodies (lenses, pods, schlieren) within the mantle section of ophiolites, orogenic lherzolites and the dunite core of Ural–Alaskan complexes.

Chromitites in layered intrusions and the mantle unit of ophiolites may rise to the rank of economic ore deposits, being the only source of chromium for industrial use. Furthermore, chromitites may carry variable amounts of

Communicated by T. L. Grove.

R. J. Baumgartner (✉) · F. Zaccarini · G. Garuti · O. A. R. Thalhammer
Department of Applied Geological Sciences and Geophysics, Montanuniversität Leoben, 8700 Leoben, Austria
e-mail: raphael-johannes.baumgartner@stud.unileoben.ac.at

platinum-group elements (PGE), being important supplier of platinum (e.g. Bushveld and Ural–Alaskan complexes). Besides their economic relevance, chromitites have become important in the geological sciences as they gained the role of petrologic indicators for their host mafic–ultramafic complexes.

Experiments and the study of natural occurrences have demonstrated that the mineral chemistry of accessory chromite from igneous rocks depends on the composition of the parental melts and can be used as an indicator of the degree of melting of their mantle source (Irvine 1965, 1967; Hill and Roeder 1974; Dick and Bullen 1984; Arai 1992; Roeder 1994; Zhou and Robinson 1994; Kamenetsky et al. 2001; Barnes and Roeder 2001). For instance, Maurel (1984; cited in Augé 1987), Maurel and Maurel (1982) and Rollinson (2008) developed calculation methods to determine the FeO/MgO ratio and the Al_2O_3 as well as TiO_2 contents of parental melts, based on the chemical composition of chromite. Moreover, compositional relations of chromite with coexisting mafic silicates (olivine, orthopyroxene) have been used to formulate geothermobarometrical methods to evaluate precipitation conditions (p, T, $\Delta \log f0_2$) of chromites in ultramafic sequences (e.g. Fabries 1979; O'Neill and Wall 1987; Ballhaus et al. 1991; Jianping et al. 1995; Liermann and Ganguly 2003, 2007). Finally, the distribution and mineralogy of PGE vary significantly according to the type of chromitite, providing invaluable information on the fertility of the mantle source from which the chromitite parental melt was extracted (e.g. Barnes et al. 1985; MacLean 1969; Keays 1995; among others). In mafic–ultramafic complexes undergoing hydrothermal alteration and weathering, chromitites may represent the only ultramafic rocks having preserved, at least in part, their original magmatic features. This is due to the higher chemical resistance of chromite compared with the associated silicates and the relative immobility of the PGE under low-temperature alteration.

The first potentially economic chromite deposit in Italy was discovered in the Bracco–Gabbro Complex (Ligurian ophiolites), close to the village of Ziona (Stella 1924). The deposit was almost completely worked out, and only a small dump is presently accessible (Brigo and Ferrario 1974). Successive exploration of the complex led to the discovery of several chromitite occurrences all of which, however, proved to be subeconomic. The Bracco chromitites are unusual compared with chromitites in ophiolite complexes of the Eastern Mediterranean Tethys, which formed in mature oceanic settings (Leblanc and Nicolas 1992). In contrast, the Bracco chromitites were emplaced in an extensional regime, during the pre-oceanic stage of the Ligurian Tethys (Lemoine et al. 1987; Piccardo et al. 2002; Piccardo and Guarnieri 2011). Formation of chromitite at spreading centres before ocean opening is uncommon (Roberts 1988; Zhou et al. 1994; Arai 1997). Therefore, knowledge of the compositional and mineralogical characteristics of the Bracco chromitites may be relevant to improve our understanding of chromitite formation in unconventional geological settings such as that of the Ligurian ophiolites.

In this study, we present a detailed mineralogical and geochemical investigation of chromitites from the same occurrences described by Bezzi and Piccardo (1970): Ziona, Mattarana, Canegreca, Cima Stronzi and Pian della Madonna. The data presented in this work include: (i) composition of fresh and altered chromite, (ii) mineralogy and composition of associated accessory minerals (sulphides and silicates) and (iii) complete set of PGE analyses on chromitites and host rocks. On the basis of the data acquired, we have calculated the possible composition of the melt in equilibrium with crystallizing chromite and have determined the conditions under which the Bracco chromitites and associated PGE might have formed.

Regional geological background

The Ligurian ophiolites and several other ophiolites in the Central and Western Alps, the Northern Apennines and Corsica represent fragments of the oceanic crust that floored the Piedmont-Ligurian Tethys. The Ligurian ophiolites have an anomalous stratigraphy compared with ideal reconstructions of the oceanic crust, since they lack a true sheeted dyke complex or a well developed cumulus transition zone. Instead, several hundred metres wide layered bodies, predominantly composed of gabbro-norite or gabbro, intruded a lherzolitic mantle characterized by a clear sub-continental petrologic signature. Pillow lavas or pelagic sediments may lie directly on the peridotite-gabbro basement. Most sections include thick horizons of ophiolitic breccia derived from seafloor erosion of plutonic and volcanic rocks (Barrett and Spooner 1977; Cortesogno et al. 1987; Lemoine et al. 1987; Piccardo et al. 2002 and references). These characters distinguish the Ligurian ophiolites from those in the eastern Mediterranean Tethys, which mainly formed in subduction-influenced geodynamic settings (Robertson 2002). The Ligurian Tethys is recognized as a magma-poor slow-spreading oceanic system (Lagabrielle and Lemoine 1997; Piccardo et al. 2002; Piccardo 2007, 2008), and, more generally, the Ligurian ophiolites have been assigned to the subduction-unrelated, Continental-margin type by Dilek and Furnes (2011). Some of the ophiolites (the External Ligurides) are actually considered to have been exhumed from continental margins along the Adriatic and the European Plates, whereas others (the Internal Ligurides) appear to have formed at a

more distal setting within the oceanic basin (Piccardo and Guarnieri 2010).

The distal mantle peridotites show widespread mineralogical and geochemical modifications due to the interaction with depleted, MORB-type asthenospheric melts percolating through the mantle by porous flow (Piccardo and Guarnieri 2010). At some stage, diffuse porous flow percolation evolved into an intrusive, channel-driven percolation mechanism giving rise to ephemeral magma chambers within the upper lithospheric mantle in which stagnant gabbroic melts underwent fractional crystallization and cumulus. The asthenospheric mantle melting happened between Early and Late Jurassic times with ages of 179 ± 9 to 164 ± 14 Ma (Rampone et al. 1998; Tribuzio et al. 2004). The peridotite-gabbro association of the Internal Ligurides underwent a polyphase tectono-metamorphic evolution from near-solidus plastic flow to low-temperature serpentinization, rodingitization and brittle fracturing during the progressive uplift from subcontinental levels to exposure at the seafloor, in Late Jurassic (Cortesogno et al. 1975, 1987).

Geology of the Bracco–Gabbro complex

Most of the information reported in this chapter is based on the official geologic map of Cortesogno et al. (1981) and the related geo-petrographic comment (Cortesogno et al. 1987), on the pioneer papers of Bezzi and Piccardo (1970, 1971), as well as on field observations made during this study. The Bracco–Gabbro Complex is located about 25 km north-westwards the city of La Spezia (Fig. 1a), between 452 km and 461 km of the ancient Roman Consular Road Aurelia, with a total exposure of about 5 × 6 km. The complex pertains to the Internal Ligurides of the Northern Apennine ophiolites and appears as a layered body intruded into partially to totally serpentinized mantle lherzolite with associated minor harzburgite and dunite. Ophiolitic breccias, pillow lavas and pelagic sediments overly the peridotites and gabbros. All rocks have been partly to completely transformed into low-temperature metamorphic assemblages dominated by serpentine, chlorite, prehnite, ferrian chromite and magnetite.

The western and northern parts of the Bracco complex are predominantly composed of gabbroic rocks (gabbro, troctolite and anorthosite). Extended layers, lenses and less regular bodies of ultramafic rocks (melatroctolite, wehrlite, dunite, chromitite) occur in the gabbroic mass, mainly concentrated along the S-E margin of the complex (Fig. 1b), possibly corresponding to the base of the magma chamber (Cortesogno et al. 1987). All rocks display an irregular tectonically disrupted layering, broadly oriented SW–NE, and defined by modal and grain-size graded bedding (Bezzi and Piccardo 1970, 1971; Cortesogno et al. 1987). Cyclic units of gabbro-anorthosite and troctolite-gabbro-anorthosite occur in gabbroic rocks, whereas dunite-wehrlite-troctolite, dunite-melatroctolite-troctolite and chromitite-melatroctolite-troctolite-anorthosite sequences characterize the internal layering of ultramafic lenses. Gabbroic and ultramafic rocks of the Bracco complex have been interpreted as a result of fractional crystallization and cumulus of a high-Mg basaltic melt, in which olivine and chrome spinel were primary liquidus phases, along with adcumulus poikilitic

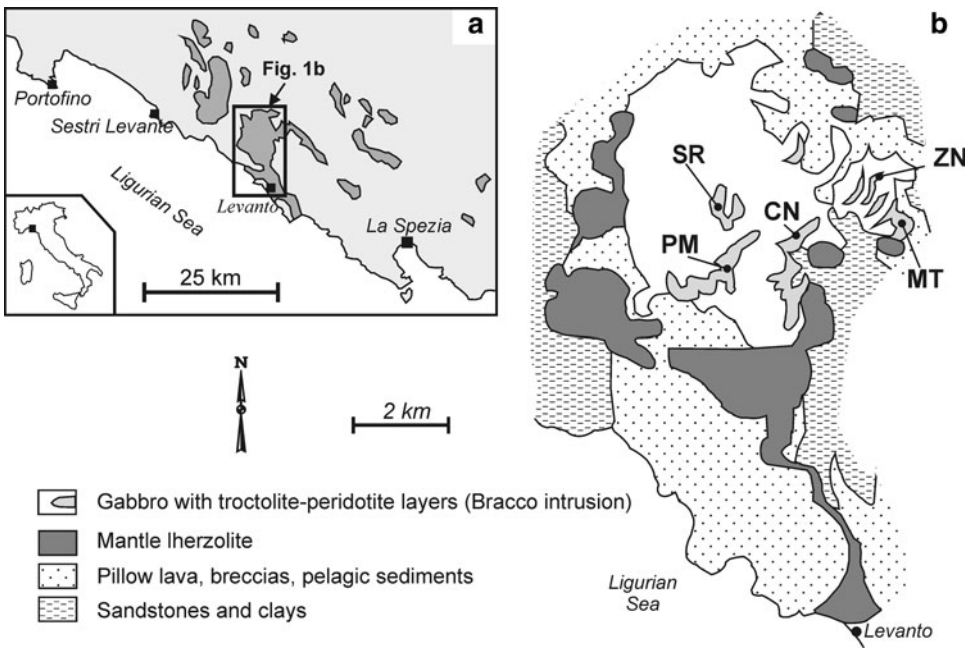

Fig. 1 **a** Sketch map with the main Internal Liguride ophiolitic bodies between Portofino and La Spezia. **b** Simplified geological map of the Bracco–Gabbro Complex (redrawn after Cabella et al. 2002) with the location of the studied areas: Cima Stronzi (SR), Ziona (ZN), Mattarana (MT), Pian della Madonna (PM), Canegreca (CN)

clinopyroxene and plagioclase varying from an intercumulus phase in troctolite to a cumulus phase in anorthosite (Bezzi and Piccardo 1970; Cortesogno et al. 1987). The layering is frequently disturbed by slumping, cross-bedding and plastic flow folding or may be truncated against irregular masses of coarse-grained gabbro and pegmatoid melatroctolite, locally characterized by harrisite texture. These textures have been reported from a number of layered intrusions all over the world and possibly reflect differential movements of a partially consolidated crystal mush or magmatic turbulence in a tectonically dynamic environment (see references in Bezzi and Piccardo 1970 and Cortesogno et al. 1987). The Bracco melatroctolites have been recently re-interpreted as a result of the interaction between lherzolite–harzburgite mantle peridotite and a silica-undersaturated melt (Renna and Tribuzio 2011).

Analytical techniques

A number of 120 polished sections were obtained from fifty samples collected at the investigated localities. Polished sections were investigated using reflected and transmitted light microscopy.

Qualitative (EDS) and quantitative (WDS) analyses as well as backscattered images of relevant textures were carried out at the Eugen F. Stumpfl Electron Microprobe Laboratory, University of Leoben, using a JEOL JXA-8200 superprobe. Measurements were performed on chromites, sulphides and silicates. For calibrations of silicate analyses, the following synthetic and natural mineral standards were used: Olivine (Si, Mg), Ilmenite (Ti), Chromite (Cr), Labradorite (Al), native Vanadium (V), Kaersutite (Fe), Rhodonite (Mn), Wollastonite (Ca), Pentlandite (Ni), Albite (Na) and Phlogopite (K). Chromite analyses were normalized on following standards: Ilmenite (Ti), Chromite (Cr, Al, Mg, and Fe), native Vanadium (V), Rhodonite (Mn) and Pentlandite (Ni). For quantitative analyses of chromites and silicates, Kα X-ray lines were used. Analytical conditions were 15 kV acceleration voltage, 10 nA beam current and peak counting times of 15–20 s per element. For Fe^{2+}/Fe^{3+} distribution, the calculation method by Droop (1987) was used. Analyses on sulphides were executed at specific analytical conditions to lower the detection limits to values of <100 ppm, which are necessary to detect trace elements (e.g. PGE). The analyses were calibrated on Millerite (Ni, S), Skutterudite (Co), Chalcopyrite (Cu), Pyrite (Fe), native Platinum (Pt), native Palladium (Pd), native Rhodium (Rh) and native Rhenium (Re). These analyses were performed with an acceleration voltage of 25 kV, a beam current of 30 nA and peak counting times of 30–60 s for trace elements (Pt, Pd, Rh) and 5–15 s for base metals (Fe, Cu, Ni, S). We used Kα, Lα and Mα X-ray lines for quantitative analyses on sulphides. Numerous chromitite samples were investigated in detail for platinum-group minerals (PGM), using reflected light and electron microscopy.

Selected rock samples were analysed for PGE and Au by instrumental neutron activation analysis (INAA), after Ni-sulphide pre-concentration with Te co-precipitation. The analyses were carried out at the University of Pavia, Italy, following the procedure described by Garuti et al. (2000), and at the XRAL Laboratories in Ontario, Canada. Average detection limits were in the order of 1 ppb for all analysed metals except Ir (d.l. < 1.0 ppb) and Os (d.l. $= 3.0$ ppb). For chondrite normalization, we used the values suggested by Naldrett and Duke (1980). Sulphur was analysed by X-ray fluorescence (d.l. $\sim$ 100 ppm). Some of the PGE whole rock analyses presented in this work were already discussed in Cabella et al. (2002).

Field relationships and petrography of selected samples

Chromitites

Chromitite samples were collected at the localities of Ziona, Cima Stronzi, Mattarana, Pian della Madonna and Canegreca (Fig. 1b). Chromitite is exclusively associated with the internal layering of ultramafic lenses, usually in close vicinity of the transition into gabbroic cumulates.

The Ziona deposit consists of swarms of centimetre- to decimetre-size pods, lenses and ribbon-like bodies, sometimes arranged in anastomosing patterns within a gangue matrix of melatroctolite. True chromitite layers are absent. However, the small ore bodies occur distributed in a tabular zone extending hundreds of metres, along the contact between the ultramafic rocks and the adjacent layered gabbros, with a maximum thickness of about 30–40 centimetres (Stella 1924; Bezzi and Piccardo 1970). The chromite may be partially altered into ferrian chromite. However, in fresh samples, chromite exhibit euhedral to subhedral crystal shape and varies in size up to 3 mm. The most common ore type consists of individual crystals closely packed in a cumulus texture, only separated one from the other by a thin film of predominant Cr-rich clinochlore and minor serpentine.

At Cima Stronzi, mafic and ultramafic rocks are clearly stratified with rhythmic repetition of melatroctolite-troctolite-anorthosite cyclic units, between 0.1 and 1.0 m in thickness (Fig. 2). The base of the cyclic units is locally marked by thin (0.5–3.0 cm) layers of olivine and chromite (dunite) or chromitite. The most common ore type consists of a centimetre-thick chromitite layer, having plagioclase as the interstitial phase in its lower part and olivine in the

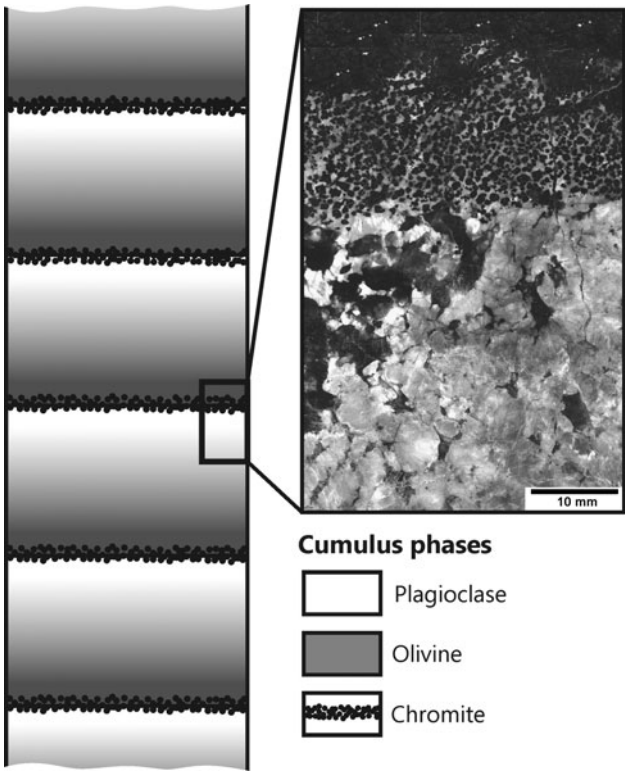

Fig. 2 Schematic illustration of the melatroctolite-troctolite-anorthosite macro-rhythmic units present at the Cima Stronzi occurrence. Chromitite layer appear at the transition between cumulus anorthosite and dunite

upper one. The plagioclase-chromitite overlies the anorthosite of the underlying unit, frequently showing wavy sharp contacts or true cusp texture (Bezzi and Piccardo 1970). Some textures appear as "load casts", suggesting that chromite settled at least a short distance in a fluid milieu and deposited over, and sunk into a less dense and partly unconsolidated material (anorthosite). The olivine-chromitite grades upwards into a dissemination of chromite grains within dunite or melatroctolite. The chromite is usually fine-grained (<2 mm) and rarely displays grain-size graded bedding. A cumulus texture is only occasionally observed, generally masked by secondary alteration. Thereby, the grains loose their original morphology, although the primary chromite is preserved by the cores of altered grains. In a second stage of alteration, ferrian chromite is replaced by a porous mixture composed of Fe oxides and hydroxides as well as silicates, probably chlorite (Fig. 3a, b).

Chromitite samples from Mattarana were collected in the Cava della Baracca and in other outcrops located a few hundred metres north of the Aurelia Roman Road. Here, the main rock is an olivine-chromite cumulate with plagioclase and pyroxene as intercumulus and adcumulus phases (Bezzi and Piccardo 1970). The most common ore type consists of an accumulation of euhedral chromite crystals, rarely exceeding 1 mm in size, within plagioclase (now transformed into prehnite) that forms the intercumulus material of large, rounded serpentinized olivine crystals up to several millimetres in size. The high-grade mineralized samples show massive chromite, filling the spaces among large olivine crystals. The true layering reported by Bezzi and Piccardo (1970) was not observed during our study. As commented by Cortesogno et al. (1987), the general structure might have resulted from syn-magmatic disruption of a semi-solid olivine-chromite-residual liquid cumulate assemblage.

Only a few samples could be collected from Pian della Madonna and Canegreca, due to the scarcity of outcrops. Chromitite layering is a common ore type at both localities, where layers may vary from 0.5 to 3–4 cm in thickness developed at the base of melatroctolite-troctolite-anorthosite cyclic units. The interstitial chromitite ore of the Mattarana type was also observed. At Canegreca, closely packed chromite aggregates form centimetre-size wispy, discontinuous vermiculations and veinlets within completely serpentinized melatroctolite (Ziona-type ore?).

Melatroctolites

The melatroctolites are medium to coarse-grained rocks that show a cumulus texture composed of partially to totally altered, subhedral olivine and poikilitic pyroxene embedded in a mesh texture of altered plagioclase (Fig. 3c). Plagioclase contents reach up to 30 wt%. The olivine cumulates are extensively serpentinized, but relics of olivine are still preserved. They contain also minor amounts of fine-grained (<1 mm), subhedral chromite, secondary magnetite and needle-shaped rutile. Coarse euhedral crystals of chromites, up to 3 mm in size, are associated with the interstitial prehnite (after plagioclase), whereas fine-grained chromite (<1 mm) occurs in poikilitic pyroxene, represented by diopside and minor augite (Fig. 3d).

Serpentinized dunites

Samples of serpentinized dunite were collected at Cima Stronzi. They are massive, dark-blue to black rocks that rarely contain plagioclase-rich veinlets. On microscale, the rocks have a diagnostic mosaic texture of olivine pseudomorphs surrounded by secondary magnetite. The rock contains mainly fresh disseminated chromites, up to several millimetres in size, with euhedral crystal shape. The chromites are usually coated and filled (along open fractures) by secondary magnetite, as a result of serpentinization.

Silicate and oxide inclusions

Chromite within the chromitite layers and the serpentinized dunites usually contains abundant silicate inclusions. The

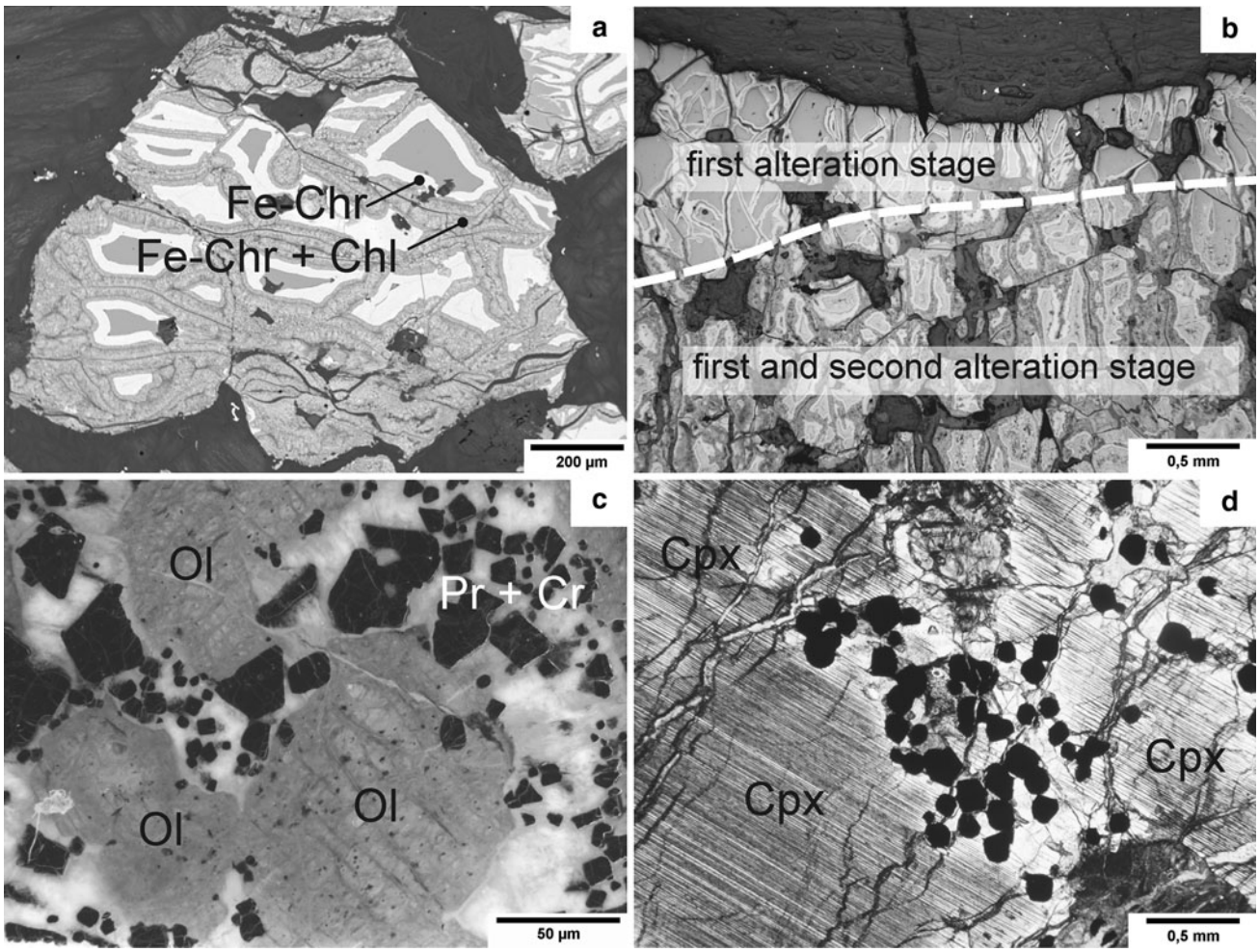

Fig. 3 **a** Backscattered electron (BSE) image showing an altered chromite that is partially replaced by ferrian chromite. The ferrian chromite rim, in turn, was replaced by a porous mixture of Fe oxides and silicates, probably chlorite. **b** Backscattered light micrograph of an intensively altered chromitite layer. **c** Thin-section photograph of an olivine-rich melatroctolite, rather euhedrally shaped chromites are associated to prehnite interstitial to altered olivine. **d** Transmitted light micrograph of disseminated chromites associated with poikilitic clinopyroxene within melatroctolite of the Mattarana occurrence. **e**, **f** BSE images of polyphase silicate inclusions in chromitite (**e**) and chromites within the serpentinized dunites (**f**). **g**, **h** BSE images of sulphides associated to the chromitites. They appear interstitially to (**g**) or as inclusions in the chromites (**h**). *An* analcime, *Ccp* chalcopyrite, *Chr* chromite, *Cpx* clinopyroxene, *Di* diopside, *En* enstatite, *Fe-Chr* ferrian chromite, *Ol* olivine, *Pn* pentlandite, *Po* pyrrhotite, *Pr* prehnite, *Prg* pargasite, *Ru* rutile

inclusions are randomly distributed with a size that ranges from a few microns up to 0.5 mm. Their shape is mainly irregular but sometimes round or even polygonal, the latter possibly representing the filling of negative crystal cavities. Inclusions in strongly altered chromites are not well preserved, showing almost complete alteration. Monomineralic silicate inclusions are rare; they are dominantly polyphase consisting of anhydrous high-T phases (olivine, clinopyroxene and orthopyroxene), hydrous high-T phases (pargasitic amphibole, phlogopite) and less common hydrous low-T phases (analcime, chlorite). Inclusions of enstatitic orthopyroxene, pargasitic amphibole, phlogopite and chlorite are common in the chromitites (Fig. 3e). Aggregates of pargasitic amphibole, olivine and diopside were observed in the chromite from dunites (Fig. 3f). The silicate inclusions may also be accompanied by oxides, such as Mg- as well as Mn-rich ilmenites and rutile. The occurrence of baddeleyite and loveringite accompanied by titanite and apatite has been reported by Cabella et al. (1997).

Sulphides

Sulphides associate with the chromitites occurring as either irregular aggregates up to 10 mm within the silicate matrix or minute (<500 µm) bleb-like grains included in fresh chromite (Fig. 3g). Pentlandite, pyrrhotite and minor chalcopyrite, locally accompanied by millerite, heazlewoodite and violarite, are the most abundant components of the interstitial sulphide aggregates. Exsolution lamellae (flame

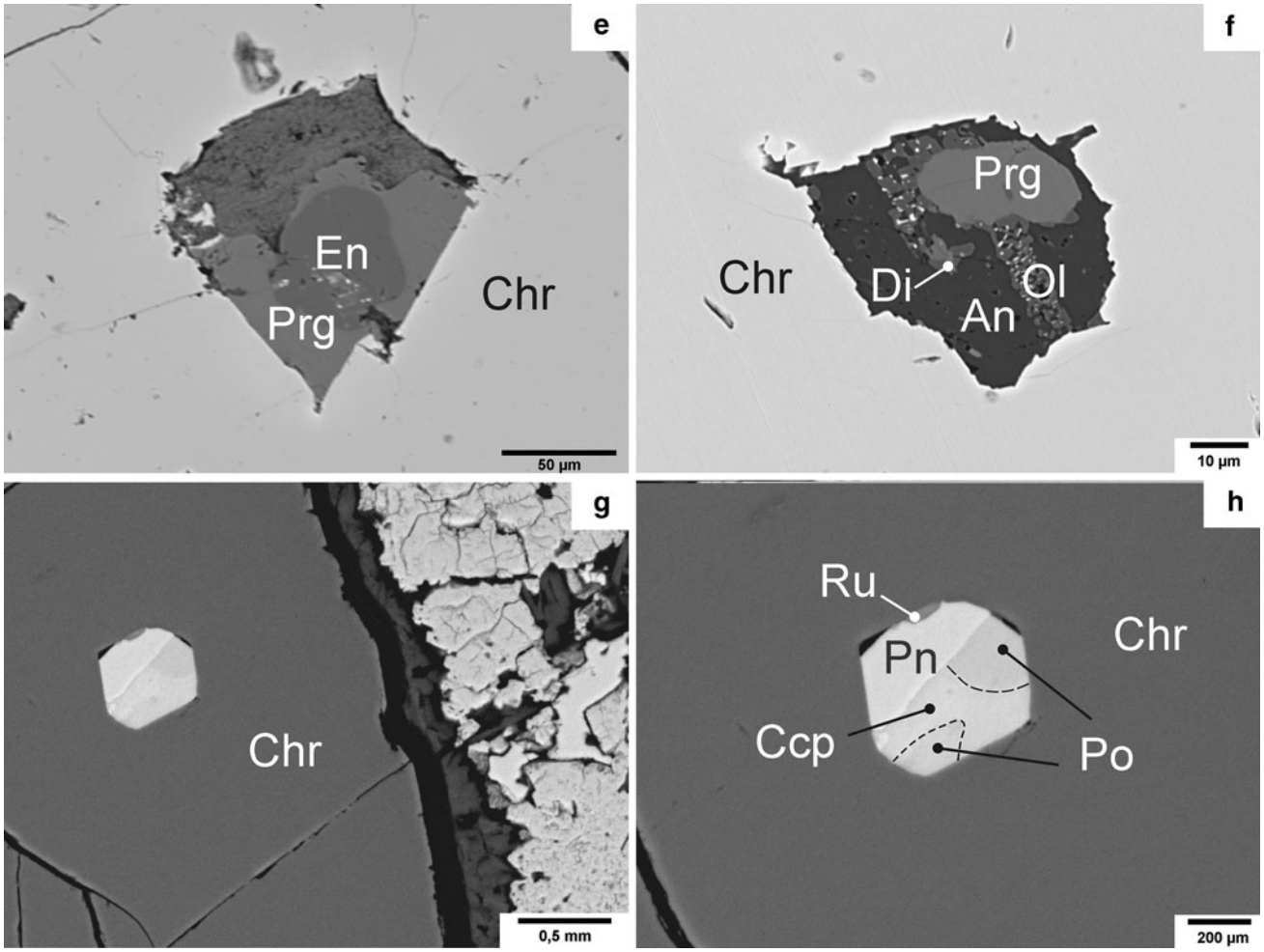

Fig. 3 continued

textured blebs or stringers) of pentlandite rarely occur in pyrrhotite. The bleb-like sulphide inclusions in chromite are polygonal or round-shaped and display variable mineral assemblages: pentlandite-chalcopyrite-pyrrhotite-rutile (Fig. 3h), chalcopyrite-millerite-bornite, chalcopyrite-pentlandite with or without pyrrhotite and mackinawite. Notably, the secondary sulphides (violarite, heazlewoodite) derived from low-temperature alteration occur exclusively in the interstitial aggregates and are absent in the blebby inclusions which were preserved from alteration by the chromite host.

Mineral chemistry

Chromite

Almost 260 microprobe analyses were performed on chromite from the massive chromitites and accessory chromite from the melatroctolites and serpentinized dunite. In chromitites, chromite composition exhibits the following variation ranges: 30.97–40.19 wt% Cr_2O_3, 22.31–31.91 wt% Al_2O_3, 17.52–24.13 wt% total iron as FeO, 11.11–15.81 wt% MgO, 0.36–0.82 wt% TiO_2, 0.12–0.38 wt% MnO and 0.06–1.00 wt% NiO. Their Mg# [Mg/(Mg + Fe^{2+})] and Cr# [Cr/(Cr/Al)] vary from 0.52 to 0.73 and 0.40 to 0.55, respectively. Therefore, most of the analyses plot in the spinel field typical of Al-rich podiform chromitites, and only a few compositions enter the magnesiochromite and chromite fields (Fig. 4a). Compositions of accessory chromite in dunite are within the ranges of the chromitites. However, accessory chromite from the melatroctolites are enriched in total FeO (25.5–38.4 wt%) and TiO_2 (0.75–1.53 wt%) and show relatively high Cr# (0.45–0.59), possibly due to re-equilibration with co-existing plagioclase. A selection of representative electron probe microanalyses on chromites is given in Table 1.

The chromitites display a broad decrease of Cr# with decreasing Mg# that is the trend expected as a result of magmatic differentiation (Fig. 4a). Furthermore, the relatively high TiO_2 content (Fig. 4b) in the Bracco chromites,

as a whole, is not consistent with typical values observed in podiform chromitites from the mantle unit of ophiolite complexes (<0.30 wt% TiO_2), but resemble more closely the high TiO_2 contents typical of stratiform chromitites. Finally, the Al_2O_3–TiO_2 relationships are consistent with spinel precipitated from a MORB-type melt, with compositions from melatroctolites being at the Al_2O_3-poor and TiO_2-rich end of the MORB field (Fig. 4c).

The calculated Fe_2O_3 content in chromite is relatively high, increasing from 6.2 wt% in chromitites, to 10.5 and 12.2 wt% in accessory chromite from dunite and melatroctolite, respectively. The chromite alteration rims are

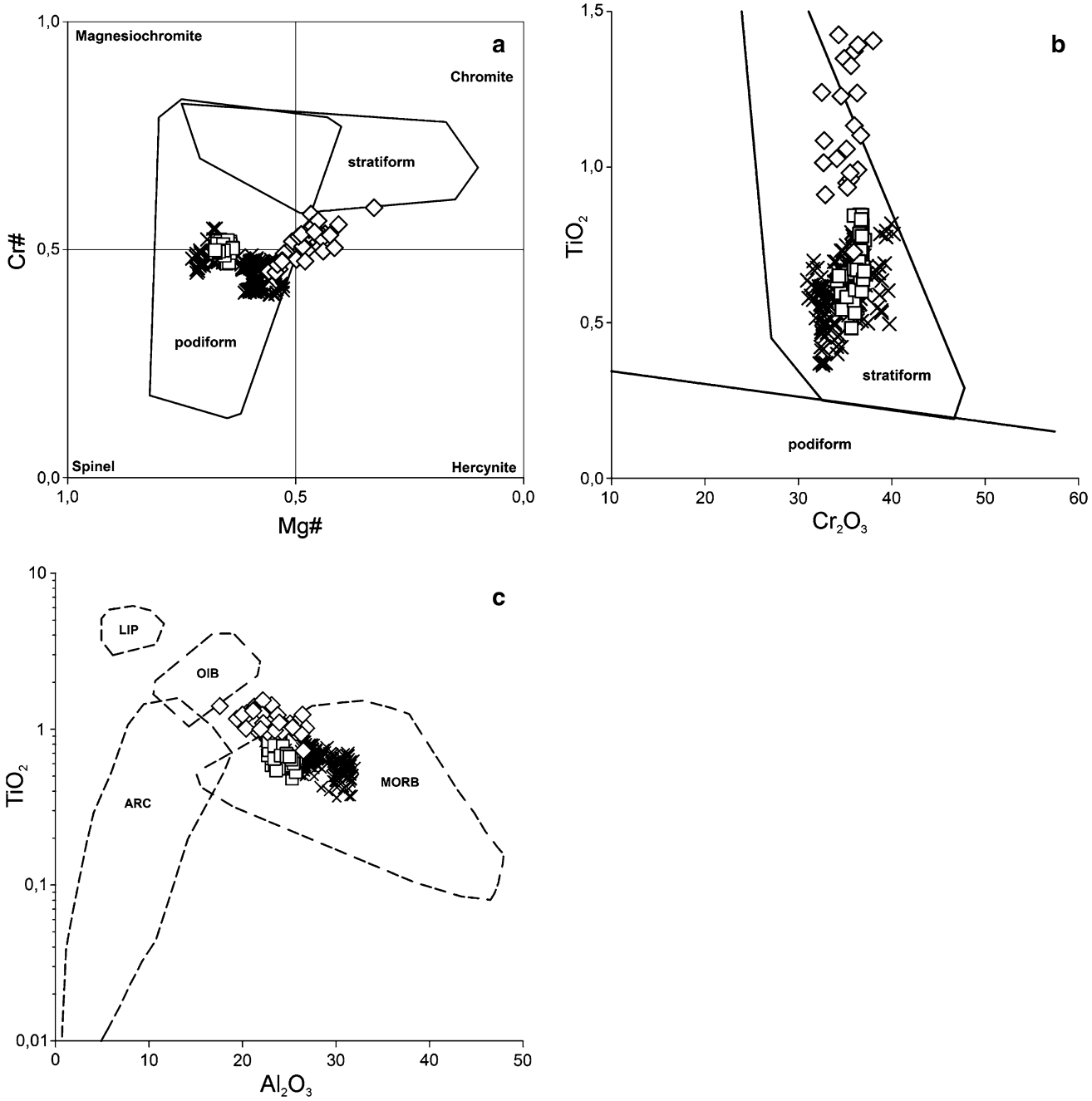

Fig. 4 **a** Classification diagram for chromites in terms of their Mg# versus Cr# (discrimination fields after Irvine 1967 and Leblanc and Nicolas 1992). **b** Composition of the chromites in terms of their Cr_2O_3 versus TiO_2 (discrimination fields after Ferrario and Garuti 1988 and Arai et al. 2004). **c** Composition of the chromites in the diagram Al_2O_3 versus TiO_2. The discrimination fields for mid-ocean ridge basalts (MORB), ocean island basalts (OIB), large igneous provinces (LIP) and island arc basalts (ARC) are derived from Kamenetsky et al. (2001). *Symbols*: cross = chromite in chromitite, diamond = chromite in melatroctolite, square = chromite in dunite

Table 1 Selection of representative electron probe microanalyses on chromites and ferrian chromite rims (wt%)

Locality	SR	SR	SR	SR	ZN	ZN	ZN	PM	PM	PM	CN	CN	CN	SR	SR	MT	MT
Rock type	Chr	Chr	Chr	Chr*	Chr*	Chr	Chr	Chr	Chr	Chr	Chr	Chr	Chr	Du	Du	Mtr	Mtr
SiO_2				3.75	3.47												
TiO_2	0.52	0.69	0.46	0.64	0.70	0.54	0.53	0.68	0.70	0.60	0.60	0.55	0.50	0.62	0.58	0.77	1.43	0.91
Al_2O_3	31.05	24.03	29.77	1.88	1.79	26.53	26.72	26.06	28.74	27.53	27.90	31.36	31.68	31.50	25.23	23.70	23.12	26.22
Cr_2O_3	31.89	39.24	34.42	33.02	33.26	38.88	38.91	38.65	35.89	35.77	36.05	32.75	32.74	32.50	35.16	37.12	34.32	32.89
V_2O_3	0.15	0.15	0.16	0.15	0.12	0.18	0.17	0.15	0.21	0.18	0.16	0.08	0.12	0.20	0.18	0.23	0.26	0.19
MgO	11.33	14.50	12.44	3.54	3.48	14.34	14.58	14.61	11.71	12.78	12.90	12.79	12.46	12.43	14.09	13.55	9.77	11.20
FeO	24.04	20.04	20.34	51.67	51.58	19.26	18.86	18.79	22.59	21.12	20.79	19.12	19.53	19.44	22.20	23.04	31.87	27.25
MnO	0.23	0.27	0.18	5.60	5.69	0.19	0.25	0.30	0.27	0.22	0.26	0.14	0.17	0.16	0.32	0.30	0.25	0.23
NiO	0.48	0.17	0.65	0.06	0.29	0.21	0.14	0.16	0.20	0.53	0.57	0.91	0.89	0.77	0.03	0.18	0.36	0.36
Total	99.69	99.09	98.42	100.31	100.38	100.13	100.16	99.40	100.31	98.73	99.23	97.70	98.09	97.62	97.79	98.89	101.38	99.25

Chr chromitite, *CN* canegreca, *Du* dunite, *MT* mattarana, *Mtr* melatroctolite, *PM* pian della madonna, *SR* cima stronzi, *ZN* ziona

* Ferrian chromite

characterized by a significant decrease of Al_2O_3 and MgO, whereas the FeO and possibly Cr_2O_3 increase. The Fe_2O_3 is extremely high, with strong increase of the Fe^{3+}/Fe^{2+} oxidation ratio indicating chromite alteration under oxidizing conditions. High concentrations of SiO_2 (up to 4.3 wt%) were detected in altered chromite rims, due to the presence of a silicate phase (possibly chlorite) filling the pores in spongy ferrian chromite. An unusual feature of the alteration pattern of the Bracco chromites is the extremely high concentration of Mn, with values up to 4.1 MnO wt% (Table 1).

Silicates

Amphiboles, pertaining to the Ca-amphibole group, are the most abundant inclusions in both the massive chromitite and the accessory chromite disseminated in the serpentinized dunite. Their Mg# ranges between 0.88 and 0.91. The Na contents are relatively high between 2.81 and 5.17 wt% NaO (Table 2). The olivine inclusions have a rather constant composition ($Fo_{89\text{-}90}$) and are characterized by nickel and calcium contents between 0.27 and 0.3 wt% NiO and 0.04 and 0.07 wt% CaO, respectively. The olivine inclusions do not differ substantially from olivine relics in melatroctolites having $Fo_{87\text{-}88}$ composition and similar contents in NiO and CaO (Table 2). Both diopside ($En_{41\text{-}43}$) and enstatite ($En_{85\text{-}89}$) inclusions contain significant Cr and Al. The poikilitic clinopyroxenes in the melatroctolites are characterized by $En_{46\text{-}49}$ (diopside) and $En_{62\text{-}66}$ (augite).

Sulphides

Electron microprobe analyses were carried out on the interstitial sulphide aggregates and some blebby inclusions within the chromite. Pyrrhotite from both types has similar compositions roughly corresponding to intermediate hexagonal pyrrhotite between the Fe_9S_{10} and $Fe_{11}S_{12}$ stoichiometry. Pyrrhotite shows variable contents of Co and Ni up to 0.25 and 1.15 wt%, respectively. Pentlandite displays compositional variations at the scale of individual samples, involving an irregular increase of the Ni/Fe ratio in the interstitial sulphide compared with the included blebs. This is interpreted as a result of exposition of the interstitial aggregates to oxidizing conditions, during serpentinization. Millerite has almost stoichiometric composition NiS, with only minor substitution of Fe up to 2.40 wt%. Violarite composition was close to stoichiometric, with similar proportion of Fe and Ni and trace amounts of Co. Chalcopyrite analyses revealed almost stoichiometric composition. A selection of representative electron probe microanalyses on sulphides is given in Table 3.

Table 2 Representative electron probe microanalyses on silicates (wt%)

Mineral Rock type	Ol Du Incl	Ol Du Incl	Ol Mtr Int	Ol Mtr Int	Di Du Incl	Di Mtr Int	Di Mtr Int	Aug Mtr Int	Aug Mtr Int	En Chr Incl	En Chr Incl	Prg Chr Incl	Prg Chr Incl	Prg Du Incl	Prg Du Incl
SiO_2	41.34	41.08	40.82	41.29	53.06	53.77	51.89	58.36	58.21	57.81	56.00	44.19	43.85	43.56	43.64
TiO_2	0.02	0.04	0.04	<d.l.	0.59	0.45	0.64	<d.l.	0.09	0.24	0.18	3.30	2.70	3.32	3.97
Al_2O_3	0.04	<d.l.	<d.l.	<d.l.	3.12	2.3	4.09	0.19	0.47	1.46	2.11	12.39	12.36	12.44	12.64
Cr_2O_3	0.54	0.51	<d.l.	<d.l.	1.42	0.03	0.08	0.12	0.07	0.75	1.09	2.33	2.17	2.61	2.44
CaO	0.06	0.05	0.04	0.03	21.62	22.78	21.68	13.32	12.33	0.23	0.33	10.68	10.97	11.13	11.03
MgO	50.42	49.7	47.9	48,00	15.21	16.96	16.07	21.59	21.89	33.39	34.50	17.76	18.06	16.51	16.37
FeO	8.13	8.55	11.45	11.80	2.69	3.26	3.47	4.79	5.22	5.88	5.68	3.43	3.49	4.17	3.85
MnO	0.19	0.19	0.20	0.22	0.04	0.10	0.11	0.09	0.12	0.17	0.16	0.07	0.10	0.06	0.03
NiO	0.27	0.32	0.24	0.22	<d.l.	0.04	0.06	0.04	0.04	0.08	0.10	0.11	0.10	0.10	0.05
K_2O	<d.l.	<d.l.	<d.l.	<d.l.	<d.l.	<d.l.	<d.l.	<d.l.	<d.l.	<d.l.	<d.l.	0.05	0.04	<d.l.	<d.l.
Na_2O	0.05	<d.l.	0.01	<d.l.	1.47	0.41	0.60	0.03	0.02	<d.l.	0.01	3.13	3.08	4.19	3.95
Total	101.06	100.44	100.7	101.56	99.22	100.1	98.69	98.53	98.46	100.01	100.16	97.44	96.92	98.09	97.97

<d.l. below detection limit, *Aug* augite, *Chr* chromitite, *Di* diopside, *Du* dunite, *En* enstatite, *incl* inclusion, *int* interstitial, *Mtr* melatroctolite, *Ol* olivine, *Prg* pargasite

Table 3 Representative electron probe microanalyses on sulphides (wt%)

Mineral	Pn Incl	Pn Int	Pn Int	Po Incl	Po Int	Po Int	Ccp Incl	Ccp Int	Ccp Int	Ml Int	Ml Int	Vio Int	Vio Int
Fe	29.78	27.77	29.89	58.86	60.69	61.00	29.69	31.45	31.97	1.87	0.87	27.42	24.98
Ni	35.50	37.72	37.81	0.48	0.48	0.41	0.29	0.01	0.11	62.55	63.76	27.32	28.33
Co	0.39	0.68	0.90	0.00	0.17	0.10	<d.l.	0.08	0.07	0.38	0.46	0.70	0.31
Cu	<d.l.	0.13	0.03	0.29	0.05	0.03	34.06	34.87	35.41	<d.l.	<d.l.	0.69	3.06
Zn	<d.l.	<d.l.	<d.l.	0.01	0.13	0.07	<d.l.	0.03	0.17	<d.l.	<d.l.	<d.l.	<d.l.
As	0.06	0.05	<d.l.	<d.l.	0.05	<d.l.	0.09	<d.l.	<d.l.	<d.l.	<d.l.	0.05	0.02
S	33.32	34.66	33.22	39.60	38.89	39.38	35.13	34.67	35.12	34.65	34.17	40.19	40.39
Total	99.05	101.02	101.86	99.24	100.46	101.00	99.26	101.10	102.85	99.45	99.25	96.36	97.08

<d.l. below detection limit, *incl* inclusion, *int* interstitial, *Ccp* chalcopyrite, *Ml* millerite, *Pn* pentlandite, *Po* pyrrhotite, *Vio* violarite

Platinum element geochemistry and mineralogy

Results of bulk-rock PGE, Au and S analyses indicate very low PGE contents between 12 and 69 ppb in the chromitites and 19–83 ppb in melatroctolites (Table 4). Total sulphur concentrations in the chromitites and melatroctolites vary between 200–5,600 ppm and 200–8,350 ppm, respectively. The melatroctolites have substantially higher Au-concentrations compared to chromitites with values up to 59 ppb. One sample of serpentinized dunite was found to contain 14 ppb total PGE, 2.5 ppb of Au and 1600 ppm of S. Chondrite-normalized PGE spidergrams (Fig. 5a, b) are very similar in all types of analysed rocks, having a deep negative anomaly in Ir, and a sharp positive slope, with remarkable enrichment of the PPGE (Pt, Pd, Rh) over the IPGE (Os, Ir, Ru). These patterns differ from those commonly observed in mantle hosted podiform chromitites that display a typical negative slope with the IPGE prevailing over PPGE. The PGE trend of the Bracco chromitites exhibits some similarity with typical trends of stratiform chromitites, except for the absence of the Rh positive anomaly and lower total PGE concentrations.

Total PGE concentrations do not correlate with S contents (Fig. 6a). However, there is a positive correlation between the PPGE/IPGE ratio and the S concentration ($R = 0.61$). This suggests that the PPGE content, in both chromitites and melatroctolites, is mainly controlled by the sulphide phase (Fig. 6b). Accordingly, with this conclusion, low PGE concentrations of Pt, Pd and Rh (Table 5) were detected in the analyses of large sulphide aggregates interstitial to chromite in the chromitites from Cima Stronzi. Pt was the most abundant PGE with concentrations up to 600 ppm in pentlandite and pyrrhotite, as well as 480 ppm in millerite. Maximum Pd and Rh concentrations

Table 4 Whole rock PGE, Au and S concentrations of selected rock samples

Locality	Rock type	Os	Ir	Ru	Rh	Pt	Pd	PGE_{tot}	Au	S
SR	Du	4.1	0.1	2.3	1.4	4.0	2.0	13.9	2.5	1,600
SR	Chr	<d.l.	0.8	<d.l.	1.1	12.6	12.1	26.6	6.2	4,400
SR	Chr	<d.l.	0.8	2.0	1.1	10.2	7.1	21.2	4.2	3,200
SR	Chr	4.0	0.7	3.0	4.0	23.0	29.0	63.7	7.0	3,100
SR	Chr	<d.l.	0.6	2.0	3.0	23.0	35.0	63.6	14.0	2,700
ZN	Chr	4.0	0.9	3.0	1.1	18.0	5.0	32.0	8.0	200
ZN	Chr	<d.l.	0.6	2.0	1.3	14.0	4.0	21.9	3.0	500
ZN	Chr	<d.l.	0.1	<d.l.	1.2	12.0	2.0	15.3	2.0	300
ZN	Chr	<d.l.	0.1	<d.l.	<d.l.	10.0	2.0	12.1	2.0	200
PM	Chr	<d.l.	0.2	<d.l.	<d.l.	11.0	3.0	14.2	3.0	300
PM	Chr	6.1	0.8	<d.l.	<d.l.	18.7	40.2	65.8	21.9	3,100
PM	Chr	4.0	0.9	2.0	2.0	11.0	6.0	25.9	3.0	700
CN	Chr	<d.l.	0.8	3.0	5.0	25.0	35.0	68.8	37.0	5,600
SR	Mtr	3.9	0.6	2.3	2.0	10.5	7.9	27.2	3.2	4,400
SR	Mtr	4.2	0.6	1.5	<d.l.	10.0	5.8	22.1	3.9	4,000
ZN	Mtr	6.0	0.7	0.9	<d.l.	27.3	47.6	82.5	22.5	8,350
CN	Mtr	<d.l.	0.7	6.5	2.6	32.1	16.0	57.9	23.8	1,760
CN	Mtr	<d.l.	1.1	6.3	2.2	31.6	17.9	59.1	25.1	1,160
CN	Mtr	<d.l.	1.1	6.1	2.7	32.0	18.1	60.0	23.1	880
MT	Mtr	<d.l.	0.1	<d.l.	2.0	10.0	7.0	19.1	6.0	1,900
MT	Mtr	4.0	0.2	<d.l.	<d.l.	14.0	7.0	25.2	3.0	900
MT	Mtr	10.5	0.5	3.5	4.1	45.9	13.1	77.6	58.3	460
MT	Mtr	9.3	0.5	3.4	4.7	37.9	12.6	68.4	58.9	680
MT	Mtr	11.0	0.4	4.0	4.0	37.0	12.0	68.4	36.0	500
MT	Mtr	13.2	0.4	3.1	4.1	34.8	12.0	67.6	47.9	200

Results are given in ppb, except sulphur (ppm)

<d.l. below detection limit, *Chr* chromitite, *CN* canegreca, *Du* dunite, *MT* mattarana, *Mtr* melatroctolite, *PM* pian della madonna, *SR* cima stronzi, *ZN* ziona

were detected in pyrrhotite with 120 and 100 ppm, respectively. The IPGE (Os, Ir, Ru) were systematically absent.

Geothermobarometry

Temperatures for chromitites were calculated on the basis of orthopyroxene inclusions in the chromites using the orthopyroxene-spinel Fe–Mg thermometry proposed by Liermann and Ganguly (2003, 2007). Calculations on almost 20 orthopyroxene-spinel pairs from the Cima Stronzi and Ziona occurrences, at an assumed pressure of 0.8 GPa, yield temperatures of 970–890 °C and 890–820 °C, respectively. Some olivine inclusions were observed in disseminated chromites within the serpentinized dunites from Cima Stronzi. Temperatures were calculated based on the olivine-spinel Fe–Mg geothermometer of Jianping et al. (1995), which is an adapted version of the thermometer developed by Fabries (1979). Five olivine-spinel pairs revealed temperatures between 900 and 820 °C. The olivine-spinel Fe–Mg geothermometer proposed by Ballhaus et al. (1991) represents a revised version of the thermometer of O'Neill and Wall (1987). Calculated temperatures, at an assumed pressure of 0.8 GPa, are in the range of 930–860 °C. However, possible subsolidus re-equilibration down to temperatures of 500 °C influences the Fe–Mg distribution between chromite and olivine (Lehmann 1983). Therefore, calculated temperatures may not reflect primary magmatic conditions, representing the possible closure of the Fe–Mg exchange reaction between olivine and chromite. Ballhaus et al. (1991) developed an olivine-spinel oxygen barometer which offers the possibility to study the oxidation state of the upper mantle based on the redox ratio $Fe^{3+}/\Sigma Fe$. Oxygen fugacities, obtained on disseminated chromites from the serpentinized dunites, fall between the QFM- and the MH-buffer with $\Delta \log fO_2$ at +2.0–2.4 units above QFM. The samples investigated in

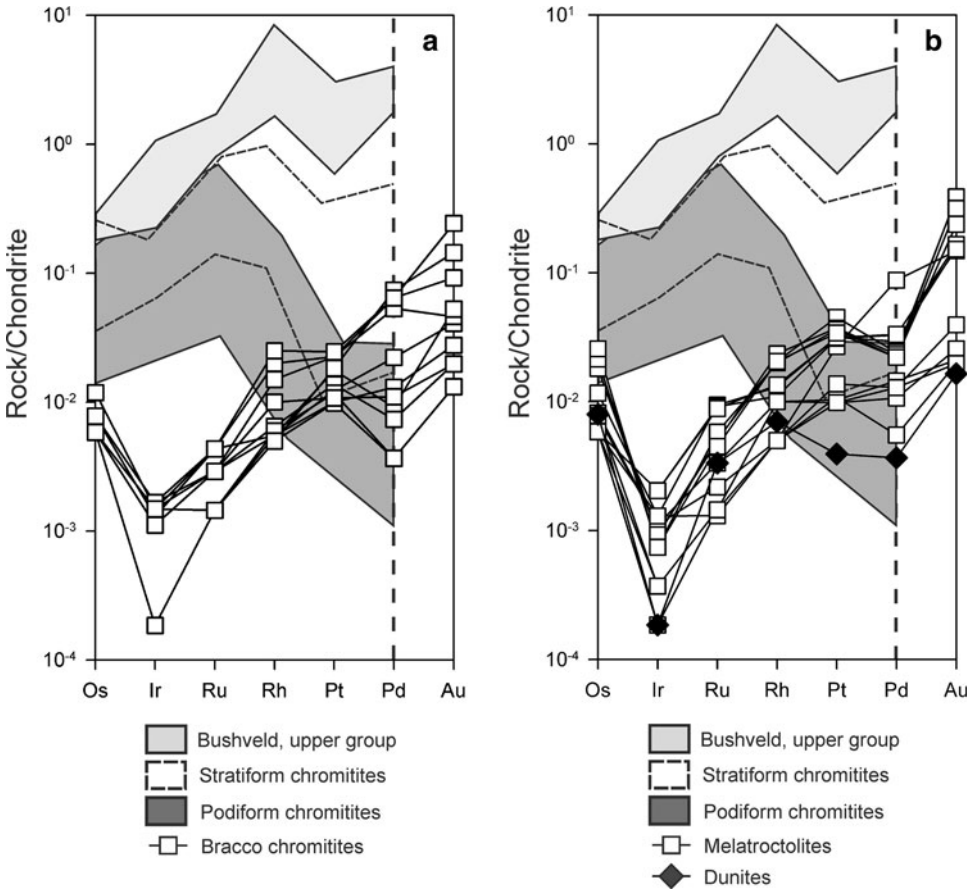

Fig. 5 **a**, **b** Chondrite-normalized PGE patterns for chromitites, dunites and melatroctolites. Normalized values were calculated after Naldrett and Duke (1980). The fields for stratiform and podiform chromitites are from Cawthorn (1999) and Zaccarini et al. (2011)

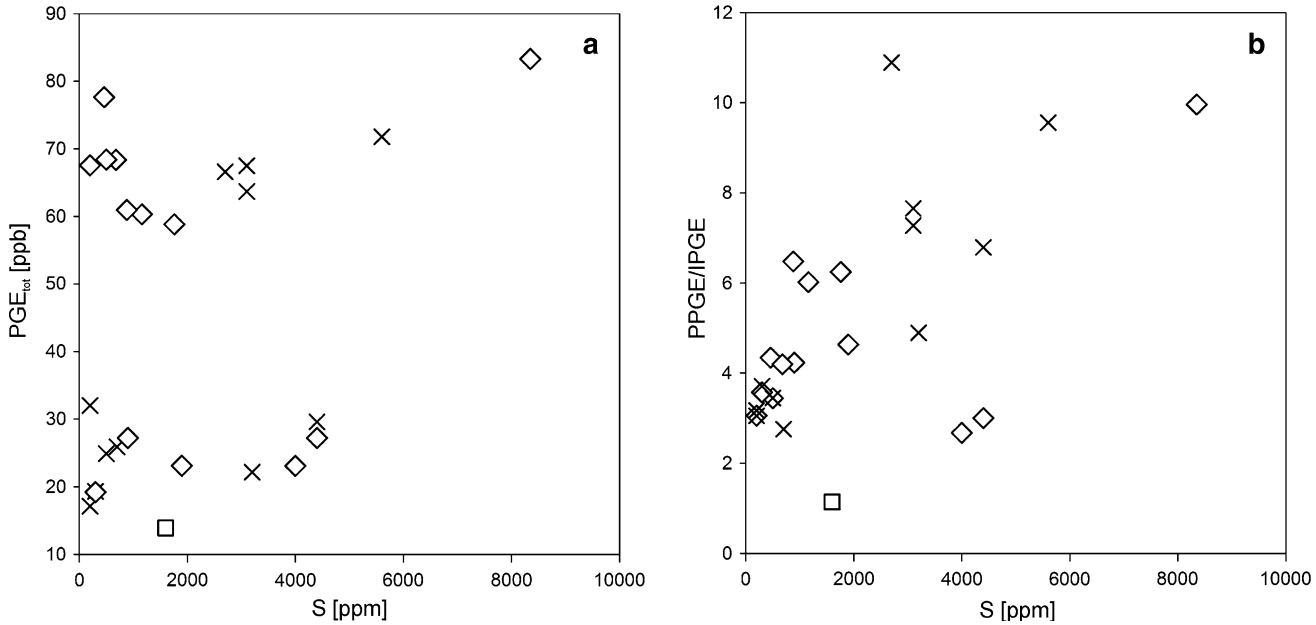

Fig. 6 **a**, **b** Whole rock PGE versus S (**a**) and PPGE/IPGE versus S (**b**) for chromitites, dunites and melatroctolites. *Symbols*: cross = chromitite, diamond = melatroctolite, square = dunite

Table 5 PPGE concentrations in selected sulphides associated with the Cima Stronzi chromitites (wt%)

Mineral	Pn	Pn	Pn	Pn	Pn	Pn	Pn	Po	Po	Po	Po	Po	Po	Ml	Ml	Ml	Ml
Pt	0.043	<d.l.	<d.l.	0.049	0.060	0.035	0.031	0.017	0.023	0.024	0.025	0.040	0.031	0.022	0.015	0.018	0.048
Pd	<d.l.	0.008	0.007	0.004	<d.l.	<d.l.	0.012	0.007	<d.l.	<d.l.	<d.l.	0.009	0.012	<d.l.	<d.l.	<d.l.	0.005
Rh	<d.l.	<d.l.	0.004	<d.l.	<d.l.	0.004	<d.l.	<d.l.	0.003	<d.l.	<d.l.	0.008	<d.l.	<d.l.	<d.l.	<d.l.	<d.l.
$PPGE_{tot}$	0.043	0.008	0.011	0.053	0.060	0.039	0.043	0.024	0.026	0.024	0.025	0.057	0.043	0.022	0.015	0.018	0.053

Ml millerite, *Pn* pentlandite, *Po* pyrrhotite

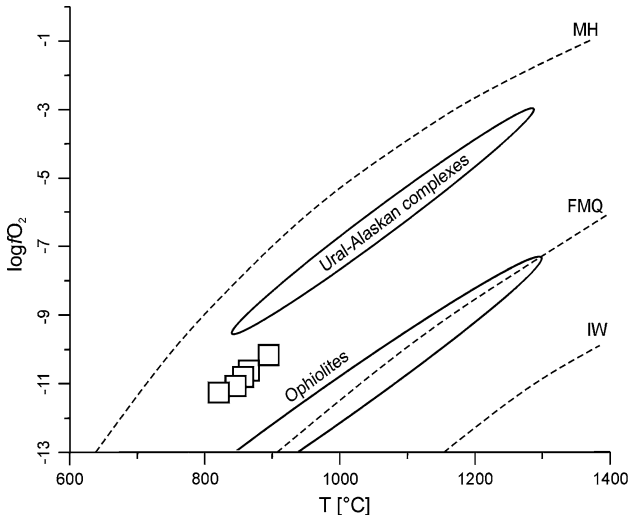

Fig. 7 Results of the olivine-spinel oxygen barometry in the plot T-ΔlogfO_2 (redrawn after Garuti et al. 2003)

this study are characterized by an oxidation state between that of chromitites from ophiolites and Ural–Alaskan-type complexes at a relatively low temperature (Fig. 7).

Parental melt compositions

The chemical composition of chromite is sensitive to the bulk chemistry of the melt from which it crystallizes. Therefore, Al_2O_3 and TiO_2 contents in the parental melt as well as the FeO/MgO ratio were calculated based on the equations of Maurel and Maurel (1982), Maurel (1984, cited in Augé 1987) and Rollinson (2008). The chromitites and the disseminated chromites in the dunite appear to have been in equilibrium with melts characterized by 14.4–16.7 wt% Al_2O_3 (Fig. 8a) and TiO_2 in the range 0.84–1.41 wt% (Fig. 8b). Calculated melt values are consistent with compositions of MORB-type magmas, in

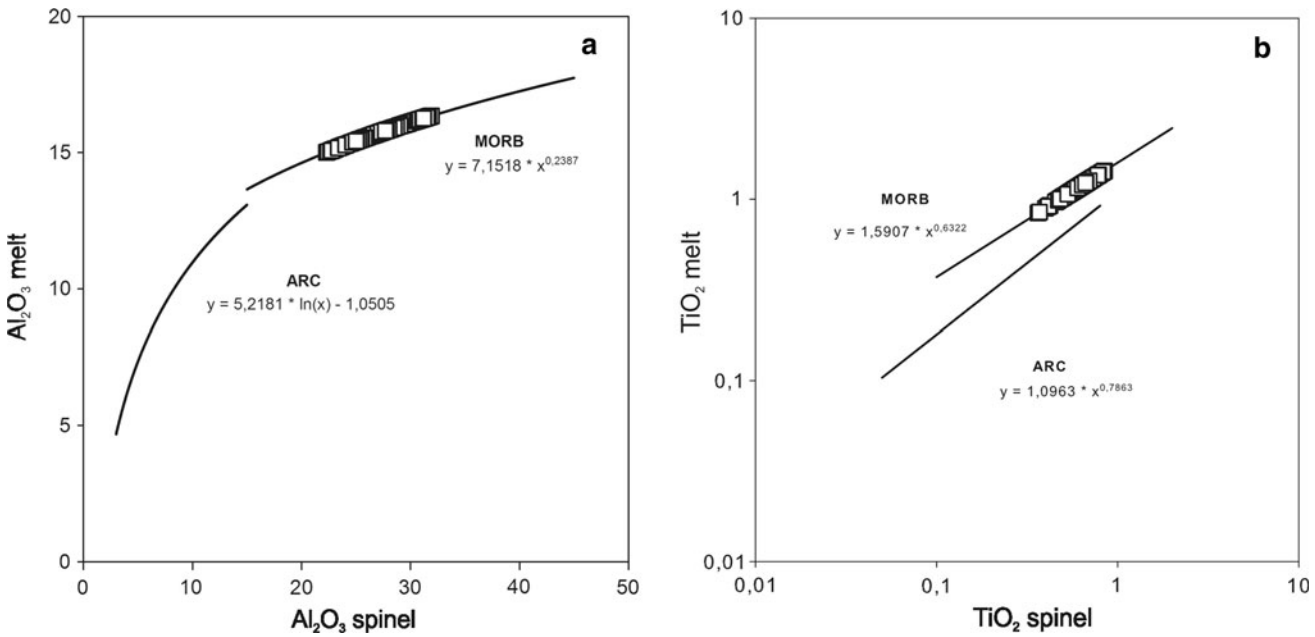

Fig. 8 **a**, **b** Calculated Al_2O_3 and TiO_2 contents in chromite parental melts. *Regression lines* for MORB and ARC lavas are derived from Rollinson (2008)

agreement with the Al_2O_3-TiO_2 relationships of the Bracco chromites presented in Fig. 4c.

The calculated FeO/MgO ratios are in the ranges 0.66–1.73 (av. = 1.19) and 0.8–0.9 (av. = 0.86) for the chromitites and accessory chromites in dunites, respectively. Some post-magmatic adjustment of the Fe/Mg ratio might have occurred in the dunites because of the high olivine/chromite volume ratio. However, this is not expected to have occurred in the massive chromitite, in which chromite Fe/Mg ratio should still reflect the composition of the parental melt.

Discussion and conclusions

The Bracco–Gabbro complex in the Ligurian ophiolites (Northern Apennine, Italy) has undergone extensive low-grade metamorphic alteration under sub-oceanic conditions that has transformed the igneous rocks (gabbros, troctolite, melatroctolite and peridotite) into prehnite-pumpellyite facies assemblages almost completely. Small partially altered chromitite bodies and rare primary inclusions in fresh chromite appear to be the only preserved phases. Geothermobarometrical data, based on chromite-orthopyroxene and chromite-olivine phase relations, indicate equilibration at temperatures between 970 and 820 °C, under relatively high oxygen fugacity above the FMQ buffer.

Constraints to the origin of the Bracco chromitites

The Bracco chromitites distinguish from podiform chromitite hosted in the mantle-tectonite of ophiolite complexes because of their different lithological association and chromite mineral chemistry (Leblanc and Nicolas 1992). Actually, they associate with predominant gabbroic rocks (vs. residual mantle peridotite and replacive dunite) and shear some structural and chemical features (stratiform morphology, high Al_2O_3, TiO_2 and Fe_2O_3) with stratiform chromitites in supra-Moho cumulate sequences of ophiolites and continental layered intrusions of the Bushveld types. However, the geological setting of the Bracco complex does not compare with either supra-Moho cumulates in ophiolites or layered intrusions in continental cratons. According to old and recent genetic models, it represents a layered gabbroic body intruding subcontinental mantle lherzolites, in an ascent spreading centre, before opening of the Piedmont-Ligurian ocean (Lemoine et al. 1987; Piccardo et al. 2002; Piccardo and Guarnieri 2011). Field relationships and internal textures of the Bracco chromitites observed in this study are consistent with the interpretation given by previous authors that the chromitites resulted from rhythmic accumulation of small amounts of chromite, during formation of the mafic–ultramafic layered zone, at the base of the Bracco magma chamber (Bezzi and Piccardo 1970, 1971; Cortesogno et al. 1987). It has been proposed that stratiform chromitites set concordant with their igneous layered host rocks, may formed by mixing of newly injected primitive melt with a more evolved residual liquid resident in the magma chamber (Irvine 1977). The objection raised that precipitation of extensive chromitite layers (e.g. Bushveld-type deposits) would require mixing of unrealistically large volumes of magma (Cawthorn and Walraven 1998) does not apply to the case of Bracco, where the volume of produced chromitite is negligible compared with the volume of the intrusion. Thus, we assume that a magma-mixing genetic model is not unrealistic for the Bracco chromitites. Fresh mafic magma, having olivine, orthopyroxene and chromite on the liquidus, was repeatedly injected in the magma chamber and reacted with the resident, more evolved residual melt. The composition of the hybrid melt was thereby shifted in the stability field of chromite as the only crystallizing phase.

As modelled by Ferreira Filho et al. (1995) and Naldrett et al. (2009), magma-mixing would also account for the appearance of an immiscible sulphide liquid during chromite precipitation that is testified by the numerous blebby inclusions of sulphide observed in almost all of the studied samples (chromitite, melatroctolite, troctolite). The predominant Fe–Ni-Cu assemblage of the blebs is consistent with on-cooling equilibration of a magmatic sulphide liquid, although the blebs might have loose some Fe by diffusion towards the enclosing chromite (Naldrett and Lehmann 1988). The large sulphide aggregates occurring interstitial to chromitite and in their host rocks indicate that the melt continued to segregate an immiscible sulphide liquid after the chromitite episode.

Significance of the PGE distribution

Podiform and stratiform chromitites are usually enriched in PGE compared to their host rocks. In particular, the podiform chromitite, with few exceptions, are enriched in IPGE. Therefore, their chondrite-normalized PGE spidergrams show a negative slope (e.g. Economou–Eliopoulos 1996; Melcher et al. 1999; Ahmed and Arai 2002). However, few examples of podiform chromitites hosted in the ophiolitic mantle (e.g. Çina et al. 2002; Escayola et al. 2011) and a number of stratiform chromitites, including the Upper Group of the Bushveld Complex (e.g. Von Gruenewaldt and Merkle 1995) display PGE positive patterns due to the predominance of PPGE over IPGE. Consistently with these two different PGE patterns, the dominant PGM in the podiform chromitite are IPGE phases, such as sulphides of the laurite-erlichmanite series, alloys in

the Ru–Os–Ir system and less abundant sulpharsenides, such as irarsite (e.g. Melcher et al. 1997; Garuti et al. 1999; Malitch et al. 2003; Kapsiotis et al. 2011). These PGM generally occur as small inclusions (<10 μm) in chromite or may partition into chromite as solid solution (Righter 2001). In the chromitites, characterized by the positive PGE patterns, two different groups of PGM have been described. The first group consists of IPGE minerals that mostly occur included in chromite. The second group is composed of PPGE minerals that generally are related to the presence of abundant sulphides in the silicate matrix of the chromitite, indicating the importance of sulphur as a collector for PPGE (Peck and Keays 1990).

The case of Bracco is rather unique because chromitites are not significantly enriched in PGE compared to their host dunite and melatroctolite. All rocks are characterized by similar concentrations and positive distribution patterns of PGE (Fig. 5a, b). Detailed mineralogical investigation failed to locate any discrete PGM inclusion in chromite. However, the low PPGE contents detected in sulphides suggest that PPGE are most likely hosted in the sulphides as solid solution or minute dispersion of atomic clusters. The broad positive correlation between bulk-rock S and the PPGE/IPGE (Fig. 6b) ratio supports the contention that the PGE distribution is a function of the original sulphide content of the igneous rocks (Naldrett and Von Gruenewaldt 1989), implying that the immiscible sulphide liquid preferentially concentrated PPGE with respect to the refractory IPGE. The fact that the IPGE and, in particular, Ir are strongly depleted in the Bracco ultramafic rocks may indicate that Os, Ru and mostly Ir were left behind in the mantle source during partial melting or were winnowed out of the magma before its emplacement. The first hypothesis is preferred because it would be consistent with generation of the Bracco parental magma by low degrees of partial melting. According to MacLean (1969), Barnes et al. (1985) and Keays (1995), a relatively large degree of partial melting, up to 30 %, is required to extract the PGE from the mantle source. Piccardo and Guarnieri (2010) demonstrated that the melts responsible for the formation of gabbroic intrusions of the Bracco type formed by relatively low degrees (4–7 %) of partial melting of an asthenospheric mantle source. This low degree of partial melting was obviously not high enough to remove all the PGE from the mantle, especially the IPGE. Only the most incompatible elements, such as sulphur and parts of the PPGE, were partially removed from the mantle and concentrated in the melt. Therefore, we can conclude that low degree of partial melting of the mantle source was the main factor to control the unusual PGE distribution in the Bracco chromitites.

Nature of the parental magma of the Bracco–Gabbro complex

According to Piccardo and Guarnieri (2011), gabbro-norite cumulates intruding ophiolitic peridotite in the Jurassic Piedmont-Ligurian basin derived from MORB-type melts whose original composition was modified by reaction with a lithospheric mantle protoliths, during ascent towards shallow upper mantle levels. Calculated melt compositions in equilibrium with the Bracco chromitites and associated dunite are characterized by 14.4–16.7 % Al_2O_3, TiO_2 contents in the range from 0.84 to 1.41 wt%, and average FeO/MgO ratios evolving from 1.19 (i.e. crystallization of chromite). These values roughly correspond to those calculated for supra-Moho cumulus chromitites in the Ural ophiolites which are believed to have crystallized in equilibrium with MORB-type melts (Garuti et al. 2012). Consistently, the S-saturation and the PGE-depleted state of the melt parental to the Bracco chromitites are features commonly observed in high-Al_2O_3 chromitites derived from MORB-type magmas (Zhou et al.1998).

The suite of solid inclusions reported from the Bracco chromitite indicates that one of the mixing magmas had relatively high water activity and carried some incompatible elements such as Na, K, Zr, Ti. In particular, Zr-bearing and REE-poor loveringite and baddeleyite have been described as “exotic” minerals in ophiolitic chromitites (Cabella et al. 1997; Renna and Tribuzio 2011). As a matter of fact, the presence of fluids enriched in Na and other incompatible elements has been reported as a common feature during the formation of ophiolitic chromitites (Johan et al. 1983), and the occurrence of Zr-bearing phases (baddeleyite, zirconolite) has been reported from gabbro-hosted high-Al_2O_3 chromitites in ophiolites of Cuba (Zaccarini and Proenza 2005). Although the possibility of fluid metasomatism during formation of the Bracco chromitites cannot be excluded in principle (Cabella et al. 1997), we suggest that enrichment in Zr could have occurred in the residual melt resident in the Bracco magma chamber as a result of extreme fractional differentiation.

Based on the Al_2O_3, TiO_2, FeO/MgO and Fe_2O_3 composition of the Bracco chromitites, we note a certain similarity with supra-Moho stratiform chromitites from subduction-unrelated continental-margin-type ophiolites of the Urals, which appear to have crystallized from tholeiitic melts, having some characteristics compatible with a sub-continental mantle source (Garuti et al. 2012).

Acknowledgments We thank the University Centrum for Applied Geosciences (UCAG) for the access to the E. F. Stumpfl electron microprobe laboratory and H. Mühlhans for the sample preparation. Many thanks are due to S. Arai and R. Tribuzio for their comments and to T.L. Grove for his editorial handling.

References

Ahmed AH, Arai AS (2002) Unexpectedly high PGE chromitite from the deeper mantle section of the northern Oman ophiolite and its tectonic implications. Contrib Mineral Petrol 143:263–278

Arai S (1992) Chemistry of chromian spinel in volcanic rocks as a potential guide to magma chemistry. Mineral Mag 56:173–184

Arai S (1997) Control of wall-rock composition on the formation of podiform chromitites as a result of magma/peridotite interaction. Resour Geol 47:177–187

Arai S, Uesugi J, Ahmed AH (2004) Upper crustal podiform chromitite from the northern Oman ophiolite as the stratigraphically shallowest chromitite in ophiolite and its implication for Cr concentration. Contrib Mineral Petrol 147:145–154

Augé T (1987) Chromite deposits in the northwestern Oman ophiolite: mineralogical constraints. Miner Depos 22:1–10

Ballhaus C, Berry RF, Green DH (1991) High pressure experimental calibration of the olivine—orthopyroxene–spinel oxygen geobarometer: implications for the oxidation of the mantle. Contrib Mineral Petrol 107:27–40

Barnes SJ, Roeder PL (2001) The range of spinel composition in terrestrial mafic and ultramafic rocks. Contrib Mineral Petrol 42:2279–2302

Barnes SJ, Naldrett AJ, Gorton MP (1985) The origin of the fractionation of the platinum-group elements in terrestrial magmas. Chem Geol 53:303–323

Barrett JJ, Spooner EFC (1977) Ophiolitic breccias associated with allochthonous oceanic crustal rocks in the East Ligurian Apennines, Italy—A comparison with observations from rifted oceanic ridges. Earth Planet Sci Lett 35:79–91

Bezzi A, Piccardo GB (1970) Studi petrografici sulle formazioni ofiolitiche della Liguria. Riflessioni sulla genesi dei complessi ofiolitici in ambiente appenninico e alpino. Rend Soc It Mineral Petrol 26:1–42

Bezzi A, Piccardo GB (1971) Structural features of the Ligurian ophiolites: petrologic evidence for the "oceanic" floor of northern Apennines geosyncline. Mem Soc Geol It 10:53–63

Brigo L, Ferrario A (1974) Le mineralizzazioni nelle ofioliti della Liguria Orientale. Rend Soc It Mineral Petrol 30:305–316

Cabella R, Gazzotti M, Lucchetti G (1997) Loveringite and baddeleyite in layers of chromian spinel from the Bracco ophiolitic unit, Northern Apennines, Italy. Can Mineral 35:899–908

Cabella R, Garuti G, Oddone M, Zaccarini F (2002) Platinum-group element geochemistry in chromitite and related rocks of the Bracco gabbro complex (Ligurian Ophiolites, Italy). 9th Intern Platinum Symp, Abstract with Program, Billings, Montana, pp 69–72

Cawthorn RG (1999) Geological models for platinum group metal mineralization in the Bushveld Complex. S Afr J Sci 95:490–498

Cawthorn RG, Walraven F (1998) Emplacement and crystallization time for the Bushveld complex. J Petrol 39:1669–1687

Çina A, Neziraj A, Karaj N, Johan Z, Ohnenstetter M (2002) PGE mineralization related to Albanian ophiolitic complex. Geol Carpat 53 (available online)

Cortesogno L, Lucchetti G, Penco AM (1975) Preorogenic metamorphic and tectonic evolution of the ophiolite mafic rocks (Northern Appenine and Tuscany). Rend Soc Ital Mineral Petrol 94:291–327

Cortesogno L, Galbiati B, Principi G (1981) Descrizione dettagliata di alcuni caratteristici affi oramenti di brecce serpentinitiche della Liguria orientale ed interpretazione in chiave geodinamica. Ofioliti 6:47–76

Cortesogno L, Galbiati B, Principi G (1987) Note alla "Carta geologica delle ofioliti del Bracco" e ricostruzione della paleogeografia Giurassico, Cretacica. Ofioliti 12:261–342

Dick HJB, Bullen T (1984) Chromian spinel as a petrogenetic indicator in abyssal and alpine-type peridotites and spatially associated lavas. Contrib Mineral Petrol 85:54–76

Dilek Y, Furnes H (2011) Ophiolite genesis and global tectonics: geochemical and tectonic fingerprinting of ancient oceanic lithosphere. Bull Geol Soc Am 123:387–411

Droop GTR (1987) A general equation for estimating Fe^{3+} in ferromagnesian silicates and oxides from microprobe analysis, using stoichiometric criteria. Mineral Mag 51:431–437

Economou–Eliopoulos M (1996) Platinum–group element distribution in chromite ores from ophiolite complexes: implications for their exploration. Ore Geol Rev 11:363–381

Escayola M, Garuti G, Zaccarini F, Proenza JA, Bedard J, Van Staal C (2011) Chromitite and platinum-group element mineralization at Middle Arm Brook, central Advocate ophiolite complex (Baie Verte peninsula, Newfoundland, Canada). Can Mineral 49: 1523–1547

Fabries J (1979) Spinel-olivine geothermometry in peridotites from ultramafic complexes. Contrib Mineral Petrol 69:329–336

Ferrario A, Garuti G (1988) Platinum-group minerals in chromite-rich horizons of the Niquelândia complex (Central Goiás, Brazil). In: Prichard HM, Potts PJ, Bowels JFW, Cribb SJ (eds) Proceedings of geo-platinum 87 symposium, Milton Keyes 1987, Elsevier, pp 261–272

Ferreira Filho CF, Naldrett AJ, Asif M (1995) Distribution of platinum-group elements in the Niquelândia layered mafic-ultramafic intrusion, Brazil: implications with respect to exploration. Can Mineral 33:165–184

Garuti G, Zaccarini F, Moloshag V, Alimov V (1999) Platinum-group minerals as indicators of sulfur fugacity in ophiolitic upper mantle: an example from chromitites of the Ray-Iz ultramafic complex (Polar Urals, Russia). Can Mineral 37:1099–1116

Garuti G, Meloni S, Oddone M (2000) NAA of Platinum group elements and gold in reference materials: a comparison of two methods. J Radioanal Nucl Chem 245:17–23

Garuti G, Pushkarev EV, Zaccarini F, Cabella R, Anikina E (2003) Chromite composition and platinum-group mineral assemblage in the Uktus Uralian-Alaskan-type complex (Central Urals, Russia). Miner Depos 38:312–326

Garuti G, Pushkarev EV, Thalhammer OAR, Zaccarini F (2012) Chromitites of the urals (part 1): overview of chromite mineral chemistry and geo-tectonic setting. Ofioliti 37:27–53

Hill R, Roeder PL (1974) The crystallization of spinel from basaltic liquid as a function of oxygen fugacity. J Geol 82:709–729

Irvine TN (1965) Chromian spinel as a petrogenetic indicator. Part I. Theory. Can J Earth Sci 2:648–672

Irvine TN (1967) Chromian spinel as a petrogenetic indicator. Part II. Petrological applications. Can J Earth Sci 4:71–103

Irvine TN (1977) Origin of chromite layers in the Muskox intrusion and other stratiform intrusions: a new interpretation. Geol 5:273–277

Jianping L, Kornprobst J, Vielzeuf D, Fabriès J (1995) An improved experimental calibration of the olivine-spinel geothermometer. Chin J Geochem 14:68–77

Johan Z, Dunlop H, Le Bel L, Robert JL, Volfinger M (1983) Origin of chromite deposits in ophiolitic complexes: evidence for a volatile and sodium-rich reducing fluid phase. Fortschr Miner 61:105–107

Kamenetsky VS, Crawford AJ, Meffre S (2001) Factors controlling chemistry of magmatic spinel: an empirical study of associated olivine, Cr-spinel, and melt inclusions from primitive rocks. J Petrol 42:655–671

Kapsiotis A, Grammatikopoulos TA, Tsikouras B, Hatzipanagiotou K, Zaccarini F, Garuti G (2011) Mineralogy, composition and PGM of chromitites from Pefki, Pindos ophiolite complex (NW

Greece): evidence for progressively elevated fAs conditions in the upper mantle sequence. Mineral Petrol 101:129–150
Keays RR (1995) The role of komatiitic and picritic magmatism and S saturation in the formation of ore deposits. Lithos 34:1–18
Lagabrielle Y, Lemoine M (1997) Alpine, Corsican and Apennine ophiolites: the slow-spreading ridge model. C R Acad Sci (Ser IIa Sci) Terre Planétes 325:909–920
Leblanc M, Nicolas A (1992) Les chromitites ophiolitiques. Chron Rech Min 507:3–25
Lehmann J (1983) Diffusion between olivine and spinel: application to geothermometry. Earth Planet Sci Lett 64:123–138
Lemoine M, Tricart P, Boillot G (1987) Ultramafic and gabbroic ocean floor of the Ligurian Tethys (Alps, Corsica, Apennines): in search of a genetic model. Geol 15:622–625
Liermann HP, Ganguly J (2003) Fe^{2+}-Mg fractionation between orthopyroxene and spinel: experimental calibration in the system FeO–MgO–Al_2O_3–Cr_2O_3–SiO_2, and applications. Contrib Mineral Petrol 145:217–227
Liermann HP, Ganguly J (2007) Fe^{2+}-Mg fractionation between orthopyroxene and spinel: experimental calibration in the system FeO–MgO–Al_2O_3–Cr_2O_3–SiO_2, and applications. Contrib Mineral Petrol 154:491
MacLean WH (1969) Liquidus phase relations in the FeS-FeO-Fe_3O_4-SiO_2 system, and their application in geology. Econ Geol 64: 865–884
Malitch KN, Junk SA, Thalhammer OAR, Melcher F, Knauf VV, Pernicka E, Stumpfl EF (2003) Laurite and ruarsite from podiform chromitites at Kraubath and Hochgrössen, Austria: new insights from osmium isotopes. Can Mineral 41:331–352
Maurel C, Maurel P (1982) Etude experimentale de la distribbution de L'aluminium entre bain silicate basique et spinelle chromifere: implications petrogenetiques, teneur en chrome des spinelles. Bull Minéral 105:197–202
Melcher F, Grum W, Simon G, Talhammer TV, Stumpfl EF (1997) Petrogenesis of the ophiolitic giant chromite deposits of Kempirsai, Kazakhstan: a study of solid and fluid inclusions in chromite. J Petrol 38:1419–1458
Melcher F, Grum W, Thalhammer TV, Thalhammer OAR (1999) The giant chromite deposits at Kempirsai, Urals: constraints from trace element (PGE, REE) and isotope data. Miner Depos 34: 250–272
Naldrett AJ, Duke JM (1980) Platinum metals in magmatic sulphide ores. Science 208:1417–1424
Naldrett AJ, Lehmann J (1988) Spinel non-stoichiometry as the explanation for Ni-, Cu- and PGE-enriched sulfides in chromitites. In: Prichard HM, Potts PJ, Bowels JFW, Cribb SJ (eds) Proceedings of geo-platinum 87 symposium, Milton Keynes 1987, Elsevier, pp 93–110
Naldrett AJ, Von Gruenewaldt G (1989) Association of Platinum-group elements with chromitites in layered intrusions and ophiolite complexes. Econ Geol 84:180–187
Naldrett AJ, Kinnard JA, Wilson A, Yudovskaya M, McQuade S, Chunnett G, Stanley C (2009) Chromite composition and PGE content of Bushveld chromitites: Part I—the lower and middle groups. Trans Inst Min Metall (Sect B: Appl Earthsci) 118: 131–161
O'Neill HSC, Wall VJ (1987) The olivine-orthopyroxene-spinel oxygen geobarometer, the nickel precipitation curve, and the oxygen fugacity of the Earth's upper mantle. J Petrol 28: 1169–1191
Peck DC, Keays RR (1990) Insights into the behaviour of precious metals in primitive S-undersaturated magmas: evidence from the Heazlewood River complex, Tasmania. Can Mineral 28:553–577
Piccardo GB (2007) Evolution of the ultra-slow spreading Jurassic Ligurian Tethys: view from the mantle. Per Mineral 76:67–80
Piccardo GB (2008) The Jurassic Ligurian Tethys, a fossil ultra-slow spreading ocean: the mantle perspective. In: Coltorti M, Grogoire M (eds) Metasomatism in oceanic and continental lithospheric mantle. Geol Soc London Spec Publ 294:11–33
Piccardo GB, Guarnieri L (2010) Alpine peridotites from the Ligurian Tethys: an updated critical review. Intern Geol Rev 52:1138–1159
Piccardo GB, Guarnieri L (2011) Gabbro-norite cumulates from strongly depleted MORB melts in the Alpine–Apennine ophiolites. Lithos 124:200–214
Piccardo GB, Rampone E, Romairone A (2002) Formation and composition of the oceanic lithosphere of the Ligurian Tethys: inferences from the Ligurian ophiolites. Ofioliti 27:145–161
Rampone E, Hoffmann AW, Raczek I (1998) Isotopic contrasts within the Internal Liguride ophiolite (N. Italy): the lack of a genetic peridotite—crust link. Earth Planet Sci Lett 163:175–189
Renna MR, Tribuzio R (2011) Olivine-rich troctolites from Ligurian ophiolites (Italy): evidence for impregnation of replacive mantle conduits by MORB-type melts. J Petrol 52:1763–1790
Righter K (2001) Rhenium and iridium partitioning in silicate magmatic spinels: implications for planetary magmatism and mantles. Lun Planet Sci 32:1759
Roberts S (1988) Ophiolitic chromite formation: a marginal basin phenomenon? Econ Geol 83:1034–1036
Robertson AHF (2002) Overview of the genesis and emplacement of Mesozoic ophiolites in the Eastern Mediterranean Tethyan region. Lithos 65:1–67
Roeder PL (1994) Chromite: from their fiery rain of chondrules to the Kilauea Iki lava lake. Can Mineral 32:729–746
Rollinson H (2008) The geochemistry of mantle chromitites from the northern part of the Oman ophiolite: inferred parental melt compositions. Contrib Mineral Petrol 156:273–288
Stella A (1924) Sopra un giacimento di cromite nel Vallone Argentiera presso Ziona (Alta Valle Vara). Boll Soc Geol It 43:183–188
Stowe CW (1994) Compositions and tectonic settings of chromite deposits through time. Econ Geol 89:528–546
Thayer TP (1970) Chromite segregations as petrogenetic indicators. Geol Soc S Afr Spec Publ 1:380–390
Tribuzio R, Thirlwall MF, Vannucci R (2004) Origin of the Gabbro-Peridotite association from the Northern Apennine Ophiolites (Italy). J Petrol 45:1109–1124
Von Gruenewaldt G, Merkle RKW (1995) Platinum group element proportions in chromitites of the Bushveld complex: implications for fractionation and magma mixing models. J Afr Earth Sci 21:615–632
Zaccarini F, Proenza JA (2005) Zirconolite from upper mantle chromitite: a key to understanding mantle metasomatic processes. Actas XVI Congr Geol Argentino 2005:346
Zaccarini F, Garuti G, Proenza JA, Campos L, Thalhammer OAR, Aiglsperger T, Lewis J (2011) Chromite and platinum-group-elements mineralization in the Santa Elena ophiolitic ultramafic nappe (Costa Rica): geodynamic implications. Geol Acta 9:407–423
Zhou MF, Robinson PT (1994) High-Cr and high-Al podiform chromitites, Western China: relationship to partial melting and melt/rock reaction in the upper mantle. Intern Geol Rev 36: 678–686
Zhou MF, Robinson PT, Bai WJ (1994) Formation of podiform chromitites by melt/rock interaction in the upper mantle. Miner Dep 29:98–101
Zhou MF, Sun M, Keays RR, Kerrich RW (1998) Controls on platinum-group elemental distributions of podiform chromitites: a case study of high-Cr and high-Al chromitites from Chinese orogenic belts. Geochim Cosmochim Acta 62:677–688